Influence of carbon black trimodal mixture on LDPE films properties: Part2 – SME

Juliano Martins Barbosa[1,2]* , Cesar Augusto Gonçalves Beatrice[1] and Luiz Antonio Pessan[1]

[1]Programa de Pós-graduação em Ciência e Engenharia de Materiais – PPGCEM, Departamento de Engenharia de Materiais – DEMa, Universidade Federal de São Carlos – UFSCar, São Carlos, SP, Brasil

[2]Engenharia de Materiais, Escola de Engenharia, Universidade Presbiteriana Mackenzie, São Paulo, SP, Brasil

*juliano.barbosa@mackenzie.br

Abstract

In this work, the influence of Specific Mechanical Energy (SME) to disperse a trimodal distribution of carbon black (CB) by extrusion was studied to evaluating the effect on LDPE films properties (colorimetric and rheological). Three types of CB were previously evaluated (PART1) and determined that the best formulation was the combination between small (S) and medium (M) particles (F18 and F13), obtaining greater tinting strength with lower viscosity. In this work (PART2), these formulations were processed with different SME levels by varying the extrusion parameters, like screw rotation speed (N) and feed rate (Q), modulate the SME. The result of each process was evaluated by Tinting Strength, MFI, Total Transmittance and it was determined that the process with 600 rpm and 10 kg/h feed rate, generating a SME of 0.29 kWh/kg for F18-P03, developed the best results, mainly in the Tinting Strength, from 126.7% to 133.2% related to F18 (PART1).

Keywords: carbon black, specific mechanical energy, tinting strength, trimodal particle size distribution, viscosity.

1. Introduction

With the production of synthetic polymers on a large scale, the need for color identification was observed, and a typical example is the colors of wires and cables, selective collection bins, and safety items, among other applications. Currently, the *Synthetic Coloring Industry* has been growing in technologies for obtaining high-performance molecules for the plastics industry because it is desired, in addition to the aesthetic appearance and identification of the materials, a contribution to the protection of the polymer matrix, in addition to the specific additives, already traditionally used[1].

Such colorants are subdivided into dyes and pigments, the latter being classified as organic and inorganic. Dyes are soluble substances in the matrix, while pigments do not dissolve and are insoluble in the polymer matrix, remaining as a distinct phase, usually with small particle size[1,2].

Among the main pigments used in polymeric materials, Carbon black (CB) is a particulate form of elemental carbon or industrial carbon. Although composed of elemental carbon, like the two crystalline forms of carbon (diamond and graphite, found in nature), CB differs chemically and physically from these pure and more crystalline forms[3].

Chemically, CB is a colloidal form of elemental carbon produced in specially designed pyrolysis reactors, operating at internal temperatures from 1400 to 2000 °C; different grades can be produced with varying particle sizes and aggregate structures[4]. The characteristics depend mainly on the manufacturing process or method, and their classification is based on this information. From a chemical point of view, the production processes for manufacturing CB are classified into two categories, the first being *Incomplete Combustion* and the second being *Thermal Decomposition* of hydrocarbons, depending on the presence or absence of oxygen. The process via incomplete combustion, termed thermo-oxidative decomposition, is the most important. In terms of production scale, the second process, the thermal decomposition of hydrocarbons in the absence of oxygen, is minimal[3]. The manufacturing methods include different processes, named according to the pyrolysis mechanisms or the raw material source, such as *Furnace Black, Gas Black, LampBlack or Thermal Black*. More than 95% of the world's annual production of CB is carried out by the *Furnace Black process*[4] and this process is illustrated in Figure 1[5].

As for the morphology of this pigment, obtained by partial combustion or thermal decomposition of hydrocarbons, it appears in the form of aggregates composed of spherical primary particles that exhibit a uniformity of sizes of primary particles within a given aggregate and turbostratic layers within the primary particles[6]. It presents a characteristic morphological hierarchy: primary particles, aggregates
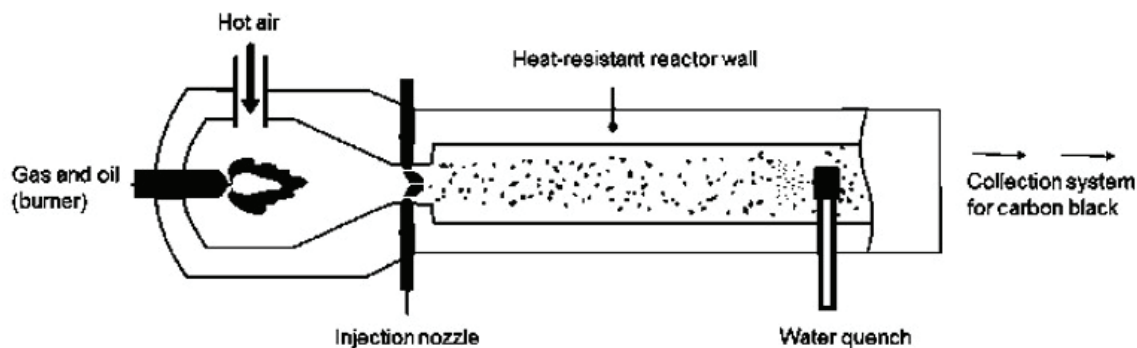
Figure 1. Schematic diagram of the combustion reactor for the Furnace Black process[5].

and agglomerates. The fundamental building block of carbon black is the primary particle and they rarely exist in isolation; however, they are solidly coalesced by covalent bonds in aggregates. Primary particles are conceptual in nature; once the aggregate is formed, the primary particle ceases to exist. Once produced, the individual aggregates are joined by secondary bonds (*Van der Waals*) to form clusters. Agglomerates do not break down into smaller components unless an adequate force (shear) is applied. The primary particle and the size of the aggregates are distributive properties and vary as a function of the CB grade[3,6]. Aggregates are robust structures capable of withstanding shear forces, the smallest units being dispersible. Agglomerates are challenging to measure accurately because they usually break when shear forces are applied.

According to the literature, primary particles exhibit a diameter ranging from approximately 10 to 100 nm and a surface area between 25 and 1500 m^2/g. When grouped, they form the characteristic units of CB, called aggregates. Many types of CB, especially those used in plastics, are subsequently converted to higher density granules for easier handling[3]. The Primary Particle size can be accurately determined only by electron microscopy, for example, via ASTM D3849[7]. However, other tests such as hue, iodine index and Nitrogen in Surface Area (NSA) via ASTM D6556[8] can also give indications of the relative size of the particles[3]. Aggregates and distribution properties are also best determined by electron microscopy; however, the absorption of Dibutylphthalate (DBPA) as per ASTM D2414[9] is also commonly used to determine the structure of CB relative to each other.

The morphology of CB is determined by the combination of the *Primary Particle* and the *Structure,* and this brings different properties and characteristics to the pigment, which directly impacts the processability of mixtures with it and its performance[10]. Depending on these CB characteristics, different morphologies may eventually be mixed to obtain specific characteristics. The first studies on bimodal packing refer to the rheological behavior of colloidal suspensions in low molecular weight matrices. These studies present relevant information about the correlation between particle size distribution and packing and how this influences the viscosity of the matrix, demonstrating that the widening of

the particle size distribution provides the highest maximum packing fraction (φ_m), resulting in lower viscosity for the same pigment content[11]. In fact, small particles have greater mobility and can move between large particles and the suspension will have a lower viscosity. The effect of fillers of bimodal size on the properties of rubber and vulcanized compounds has few studies; however, one of them refers to the effectiveness of the insertion of iron particles in the excluded volume of silicone rubber with a bimodal size distribution, and it was observed that mixtures of carbon blacks or any fillers could improve the performance of composites compared to a single distribution composite, correlating the positive results in the quality of the filler dispersion. Therefore, a more accurate assessment of particle packing and its effect on the properties of polymeric compounds is needed[11].

When carbon black particles are incorporated into the polymer, there is an intense interaction between the matrix and the pigment structure, such as physical adsorption on the surface of the carbon black particles. The greater the surface area or structure of the pigment, the greater the interaction between them, and the greater the limitation of the mobility of the chains; that is, the relaxation times will be longer[12].

The rheological measurements commonly used in polymer characterization are the Rheological Properties in Shear Steady State. The measurements are obtained under shear flow, where the velocity has only the component in the flow direction. When a polymer is subjected to a given shear rate, it will present a resistance to flow, indicated by the quantity known as the steady-state shear viscosity, $\eta(\dot{\gamma})$. This is one of the most important rheological properties in the processing of molten polymers. The flow rates, pressure drops, and temperature increases, which are important parameters in these operations, directly depend on this property[12].

On the other hand, the Rheological Properties in Shear Oscillatory State are measured using a small amplitude oscillatory shear strain, in which the applied shear stress (or strain) varies at a given frequency. The magnitude of the strain must be small enough to ensure that the measurements fall within the linear viscoelasticity regime. As molten polymers are viscoelastic (they have a response composed

of an elastic and a viscous part) and the stress (strain or stress) is of small amplitude, the response (stress or strain) will oscillate with the same frequency; however, it will be out of phase into the load, exhibiting a linear viscoelastic behavior[12,13].

In this way, Zhang et al.[14] determined the rheological behavior of HDPE composite filled with CB at low shear rates under constant temperature. The results indicate the correlation between the dispersed pigment and the polymer matrix. At a sufficiently high filler concentration, a structural skeleton appears to form, which significantly increases the modulus, particularly at low frequencies. The large structure and small primary particle size of CB significantly increase the modulus of elasticity, more than the small structure and larger particle size, for example, an N550, classified according to ASTM D 1765[15]. Oxidized CB increases the modulus of elasticity in the entire frequency region due to the greater interaction between the pigment and the polymer matrix[14].

Regarding particle packing, Aghajan et al.[11] studied bimodal mixtures of CB, type N220 and N550, with different average particle sizes but similar structures. The maximum packing density in the CB blend was achieved in the 35/65 composition of N220 / N550. In addition, some properties of non-vulcanized compounds, such as bulk density, rheometry and non-linear viscoelasticity, showed synergistic effect when the rubber was filled with this bimodal mixture. It is observed that the bimodal mixture of CB forms a packed or network structure with a short distance between particles in which the macromolecules are highly immobilized, playing an essential role in the density and rheological properties of the compounds. This phenomenon was absent in the vulcanized state of the compounds due to the degree of vulcanization and chemical crosslinking density in the rubber; however, such properties were improved as a function of the packing of the particles[11].

Therefore, studying the packing and distribution of particles and how this behavior influences the rheological properties of a composite or nanocomposite is of fundamental importance for the understanding its processability characteristics and the relationship between its structure and properties, in addition to providing information about the distribution and dispersion of particles in the polymer matrix, which directly affect and influence the processing characteristics and interfering with the colorimetric performance of the composition.

2. Materials and Methods

2.1 Materials

The inorganic pigment (Carbon black - CB) was identified as *Black Pearls* 900 (Small - S), Regal 99I (Medium - M) and Black Pearls 120 (Large - L), all supplied by Cabot

Corporation (USA), according to Table 1[16] and dispersed at 30% loading in low density polyethylene (LDPE) grade PB608[17], with MFI of 30 g/10min (2.16 kg@190 °C) or 65 g/10min (5.00 kg@190 °C) produced by Braskem (Brazil).

2.2 CB concentrates preparation

Using the best formulation previously defined in PART 01, identified as **F18 (25/75/00)** and **F13 (75/00/25),** extrusion parameters were varied to improve concentrate dispersion in a twin-screw extruder by Specific Mechanical Energy (SME) of the process according to screw rotation speed **(N)** and feed rate **(Q)** in a ZSK18 (*Coperion GmbH*) with L/D 48 (same screw profile shown in part01), maximum power of 4 kW (5.43 hp), maximum amperage of 15.2 A, maximum screw rotation speed of 600 rpm and maximum feed rate of 140 kg/h by the main feeder (without using side feeder) and thermal profile between 120 and 180 °C. The parameters associated with the SME are presented in Equation 1[18,19].

$$SME = \left(\frac{\frac{N_0}{N_{max}} \times W_{max} \times \frac{T}{100}}{Q} \right) \qquad (1)$$

where, SME = Specific Mechanical Energy (kWh/kg), N_0 = extruder screw rotation speed (rpm), N_{max} = maximum extruder screw rotation speed (rpm), W_{max} = maximum power of the extruder engine (kW), T = extruder torque (%) and Q = feed rate (kg/h).

To obtain different levels of SME and vary its value, two values of extrusion screw rotation speeds (N) and two values of feed rates (Q) were used, as shown in Table 2.

The screw elements profile extruder was based on information available in the literature[20,21]; however, there was a need for adaptation due to the difference in L/D between the extruders.

2.3 Dilution of CB concentrates

For some tests, measurements were done in a polymeric film and the specimens were prepared by blow mold extrusion (thickness 40 μm and blowing ratio of 1:3) with dilution at 5% in LDPE (MFI 2 g/10min).

2.4 Characterizations

2.4.1 Composition characterization

The CB content in the samples was determined via gravimetric after pyrolysis at 600 °C in a nitrogen atmosphere and then in a regular atmosphere, following the ASTM D1603[22].

Table 1. Principal properties of carbon black[16].

Properties	Unit	Standard	BP 900 (S)	Regal 99I (M)	BP 120 (L)
Primary particle	nm	ASTM D3849	15	38	75
Oil absorption (OAN)	cc/100g	ASTM D2414	64	63	64
Nitrogen Surface Area (NSA)	m²/g	ASTM D6556	230	62	25
Tinting Strength	%	ASTM D3265	151	97	58

2.4.2 Rheological properties characterization of CB concentrates

The MFI, which is a basic determination of the rheological behavior of compositions, was determined according to ASTM D1238 (5.00 kg@190 ºC)[23]. Subsequently, the rheological properties were determined at low (parallel plates) and high (capillary) shear rates. The Complex Viscosity (η^*) as a function of angular frequency (ω) was determined in a rheometer ARES from Rheometric Scientific (N_2 atmosphere, 210 °C, parallel plates geometry with a diameter of 25 mm and 1 mm of gap) with a frequency range between 10^{-2} and 10^2 rad.s^{-1} and a constant strain of 1% (linear viscoelastic region). The behavior at high shear rates was obtained by capillary rheometry in an Instron rheometer, model 4467 (Lc = 24.384 mm, Dc = 1.270 mm, Lc/Dc = 20 at 210 °C) with a shear rate range between 10^1 and 10^4 s^{-1} which is equivalent to the values found in a twin-screw extrusion process[12].

2.4.3 Colorimetric and optical properties characterization

The tinting strength is a quantitative method for comparing pigment performance to a reference. Prepared by mixing one part of CB concentrate (black) with ten parts of titanium dioxide pigment (white) – 1:10, generating a gray color. The more intense this gray, the greater the tinting strength of CB, as it stands out over white. On the other hand, the less intense the gray, the lesser the tinting strength because the white pigment stands out from the CB. The quantitative determination was performed in a spectrophotometer Datacolor (SF 600), using *Contrast Ratio* mode, calculated by the CIE LAB L*a*b system[24]. For Total Transmittance (TT), measured in film specimen, which physically represents the total incident light and transmitted through the sample, being reduced by the reflectance or absorption of light by the sample, measured using a BYK Gardner spectrophotometer (Haze-Gard Plus), following ASTM D1003 standard, operating in transmittance mode[25-27].

2.4.4 Dispersion and microscopy characterization

The state of the dispersion was evaluated by two techniques: the first (quantitative) via the Filter Pressure Value (FPV) and the second (qualitative) by Optical Microscopy (OM), observing the agglomerates dispersed in the polymer matrix. The FPV evaluates the degree of dispersion of pigments through a standardized screen filtration mounted on an extruder and this filtration generates retention of undispersed pigment particles. The degree of dispersion can be quantified by the pressure variation, according to EN-13900[28], using #635 mesh (15 μm), 220 °C and 200 g of concentrate. The OM was used to observe the CB microdispersion in the film specimen using a Leica microscope (DMRXP) and the images were captured with Image Pro Software at 400x magnification.

3. Results and Discussions

In PART 1 of this study, the best CB combination was identified, F13 (75/00/25) and F18 (25/75/00), prepared in a twin-screw extruder, using 300 rpm@20 kg/h, resulting in the best dispersion, with the highest possible tinting strength and maintaining the lowest viscosity. In this PART 2, SME Extrusion was used to improve the dispersion, according to Table 3.

F13 (75/00/25) and F18 (25/75/00) samples were evaluated in independent groups for better observation of the process variables and the balance between the colorimetric properties and viscosity of the formulation. As the desired result, the lowest possible FPV, higher Tinting Strength and higher MFI are expected to maximize the colorimetric properties with the lowest viscosity for processing. Regarding F13 (75/00/25) results, best values from Tinting Strength and FPV were obtained with N of 600 rpm and Q of 10kg/h in the formula F13-P03 with 124.8% and 15.4 bar, respectively. The colorimetric effect with the increase in tinting strength can be observed in the Ref. (F17) x Result columns, showing the darker gray. The highest MFI was obtained with the same Q but with an N of 300 rpm, resulting in 14.7 g/10min in F13-P01. The same trend was observed in the behavior of the

Table 2. Processing parameters for SME modulation.

Process	N (rpm)	Q (kg/h)
P01	300	10
P02	300	20
P03	600	10
P04	600	20

Table 3. Results of the main characterization tests.

Sample	N (rpm)	Q (kg/h)	SME (kWh/kg)	CB content (%)	MFI (g/10min)	Tinting Strength (%)	Ref. (F17)	Result	FPV (bar)	TT (%)
F13-P01	300	10	0.15	29.6	14.7	114.9			22.1	10.7 ± 0.8
F13-P02	300	20	0.10	28.5	9.2	122.3			20.3	8.1 ± 0.7
F13-P03	600	10	0.28	30.2	7.2	124.8			15.4	7.5 ± 0.7
F13-P04	600	20	0.16	29.9	9.4	120.7			17.4	9.2 ± 0.6
F18-P01	300	10	0.14	29.6	23.4	129.4			1.5	7.2 ± 0.4
F18-P02	300	20	0.09	30.3	19.7	127.3			1.6	7.5 ± 0.5
F18-P03	600	10	0.29	30.2	16.2	133.2			1.5	5.7 ± 0.8
F18-P04	600	20	0.16	29.8	18.1	124.4			1.7	8.5 ± 0.9

results for F18 (25/75/00), that is, higher Tinting Strength and lower FPV obtained 600rpm and 10kg/h, with the formula F18-P03 with 133, 2% and 1.5 bar, respectively. Visually, the colorimetric effect obtained by the increase in the tinting strength is more intense, as evidenced by the difference in tones observed between the Ref. (F17) x Result columns. The highest MFI was obtained with the same Q but with 300 rpm, resulting in 23.4 g/10min in the F18-P01. These behaviors in results can be observed in Figure 2 in the form of Misture Contour Graphics.

In Table 3, it is shown the correlation between the Total Transmittance (TT) and the Tinting Strength; thus, the greater the tinting strength, the lower TT because the pigment dispersed in the matrix, in addition to providing coloration, also reduces the passage of light in the substrate. This correlation is observed graphically in Figure 3.

Evaluating the Complex Viscosity of the samples, it is observed that the difference in the profile of the curves was discrete and there was almost no variation between the curves of F13-P01 and F13-P03, which represent the extreme values of MFI. Subtly, F13-P03 showed higher viscosity than F13-P01, probably due to the higher SME in the process, which resulted in better pigment dispersion in the matrix, as observed in increased tinting strength and reduced FPV. The same logic applies to sample F13 (75/00/25). Regarding the F18 group, it is observed that the variation

in processing did not bring significant differences between F18-P01 and F18-P03; however, both had lower viscosity than F18 (25/75/00) with an increase in Tinting strength, which went from 126.7% to 133.2% but the FPV had a slight increase, going from 1.2 bar to 1.5 bar. This is due to a more efficient process, which dispersed the pigment better, increasing the Tinting strength without interfering with the viscosity of the system, as presented in Figure 4.

At high shear rates, the curves produced in capillary rheometry are shown in Figure 5. As observed, even at high rates, the rheological profile of viscosity remained close until 10^3 s^{-1}; however, we have two very different groups of samples depending on the formulation, that is, the F13 group, with higher viscosity, with emphasis on F13 (75/00/25) and F13-P03, with values higher than F13-P01 due to the higher SME used in the process and which resulted in better pigment dispersion and consequent increase in tinting strength. In the F18 group, with lower viscosity, F18 (25/75/00) and F18-P01 showed similar behavior, while F18-P03 had a slightly higher viscosity than the others; however, it developed a significant increase in Tinting strength (133.2%) with low FPV (1.5 bar).

In Table 4, it is shown the Power Law Index (n) of the curves obtained by capillary rheometry, indicating the pseudoplasticity. Broadly, the F13 group showed greater pseudoplasticity than the F18 group. The formula F13-P01 presented n of 0.435,
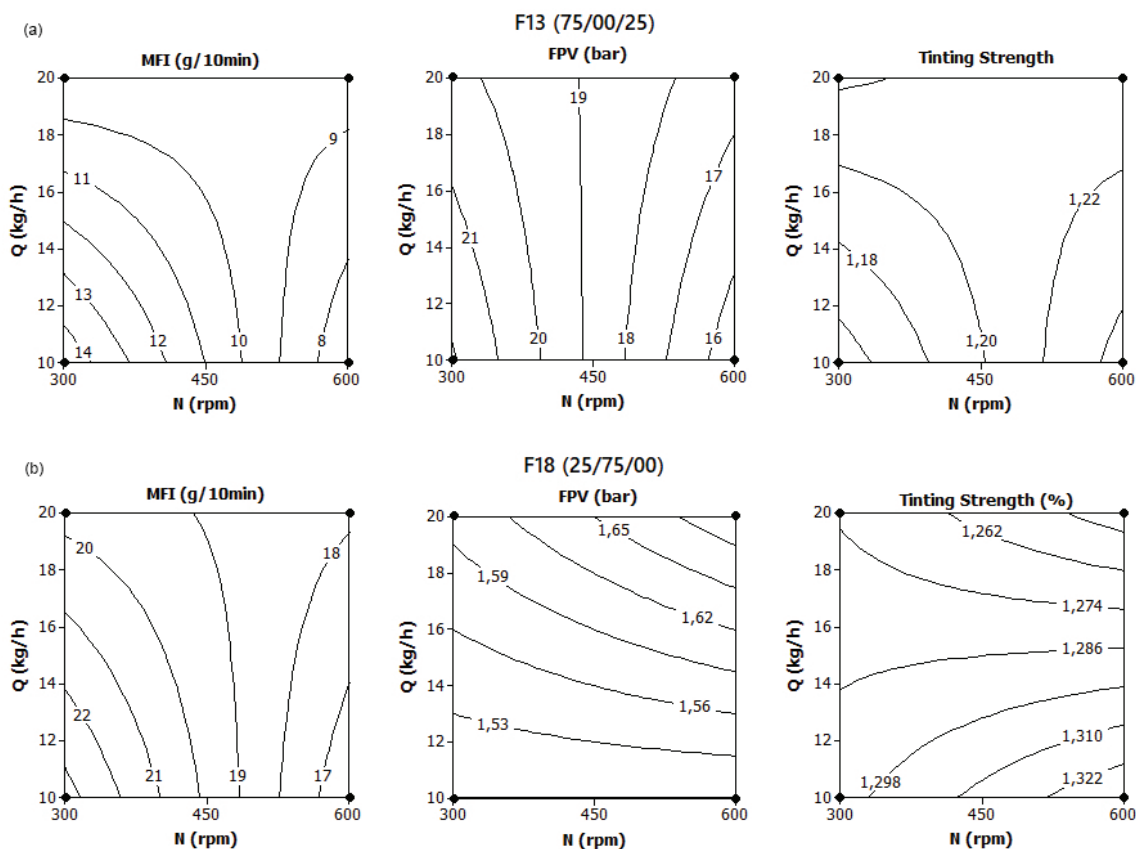

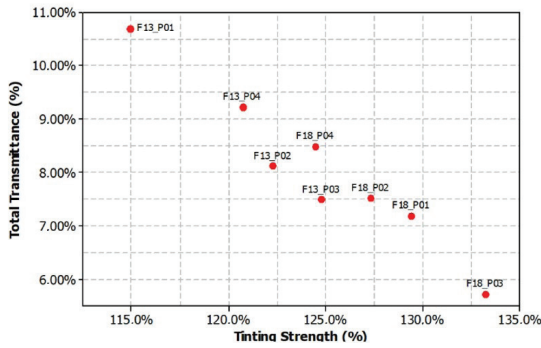**Figure 2.** Mixture Contour Graphics of MFI, FPV and Tinting Strength for F13 (a) and F18 (b) groups.

Figure 3. Correlation between Tinting strength and total transmittance (TT).

Figure 4. Complex Viscosity of F13 (a) and F18 (b) groups.

Figure 5. Viscosity at high shear rates of F13 and F18 groups.

Table 4. Power Law Index at high shear rates - F13 and F18 group.

Sample	N (rpm)	Q (kg/h)	FPV (bar)	Tinting stregth (%)	n
F13 (75/00/25)	300	20	14	113.9	0.379
F13-P01	300	10	22.1	114.9	0.435
F13-P03	600	10	15.4	124.8	0.413
F18 (25/75/00)	300	20	1.2	126.7	0.484
F18-P01	300	10	1.5	129.4	0.506
F18-P03	600	10	1.5	133.2	0.469

which showed less pseudoplasticity than the F13-P03, with 0.413. The latter developed greater tinting strength. This is probably due to the more significant interaction between the matrix and the S pigment obtained by the better dispersion with increasing SME.

On the other hand, F18-P01 presented an n of 0.506 while F18-P03 had an n of 0.469, emphasizing that F18-P03 developed greater tinting strength, with lower viscosity and less pseudoplasticity, which represents easiness in processing and a better distributed pigment in the matrix. It also indicates that this process was able to disperse the pigment very well in the matrix, with no changes in viscosity at high rates.

The Specific Mechanical Energy (SME) used in each processing, which was modulated as a function of the rotation speed of the extruder screw (N) and the feed rate (Q) in the processes and monitored by the Torque (%) of the extruder motor, shows that the best dispersion results, leading to an increase in tinting strength, were obtained with higher levels of SME, as shown in Table 3.

The above results are better explained in the OM micrographs below, which illustrate the clusters present in the films. It is observed that the P01 process (300 rpm@10 kg/h) was less efficient in the dispersion of CB, with the presence of a greater number of agglomerates due to the lower SME used in the processing. (0.14 and 0.15 kWh/kg). The P03 process (600 rpm@10 kg/h) produced a smaller number of agglomerates and a greater Tinting Strength, as discussed above and presented by the images in Figure 6.

Evaluating all the results presented, it is observed that the best results in Tinting strength and FPV were obtained with the use of the highest SME in the process, that is, values of 0.28 kWh/kg for F13-P03 and 0.29 kWh/kg for F18-P03, both used 600 rpm of rotation speed (N) and 10 kg/h in feed rate (Q). As for the formula variable, that is, the performance response of each of the mixtures as a function of the process, F18 (25/75/00) presented higher Tinting strength and lower FPV than F13 (75/00/25), as shown earlier in the results. In the rheological effect, an increase in viscosity was observed as a function of the increase in SME. However, the lowest impact was obtained with F18 (25/75/00) observed in the Complex Viscosity curves presented. In this way and based on the results presented above, the formula that followed for PART 03 was F18-P03.
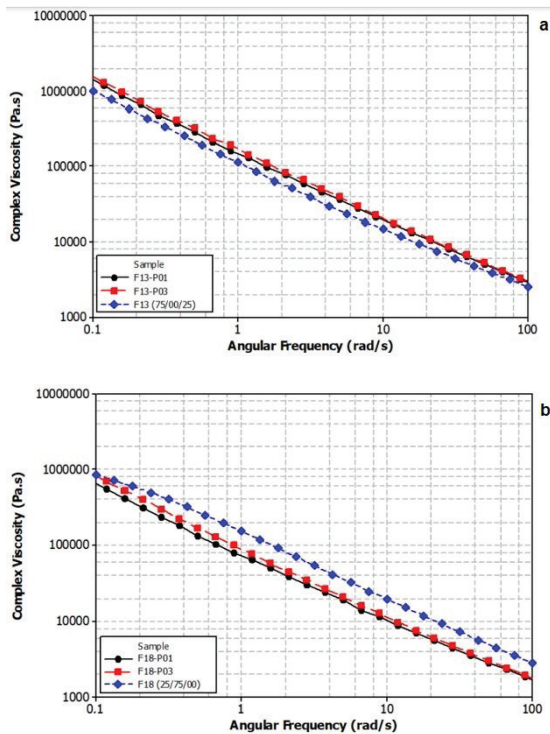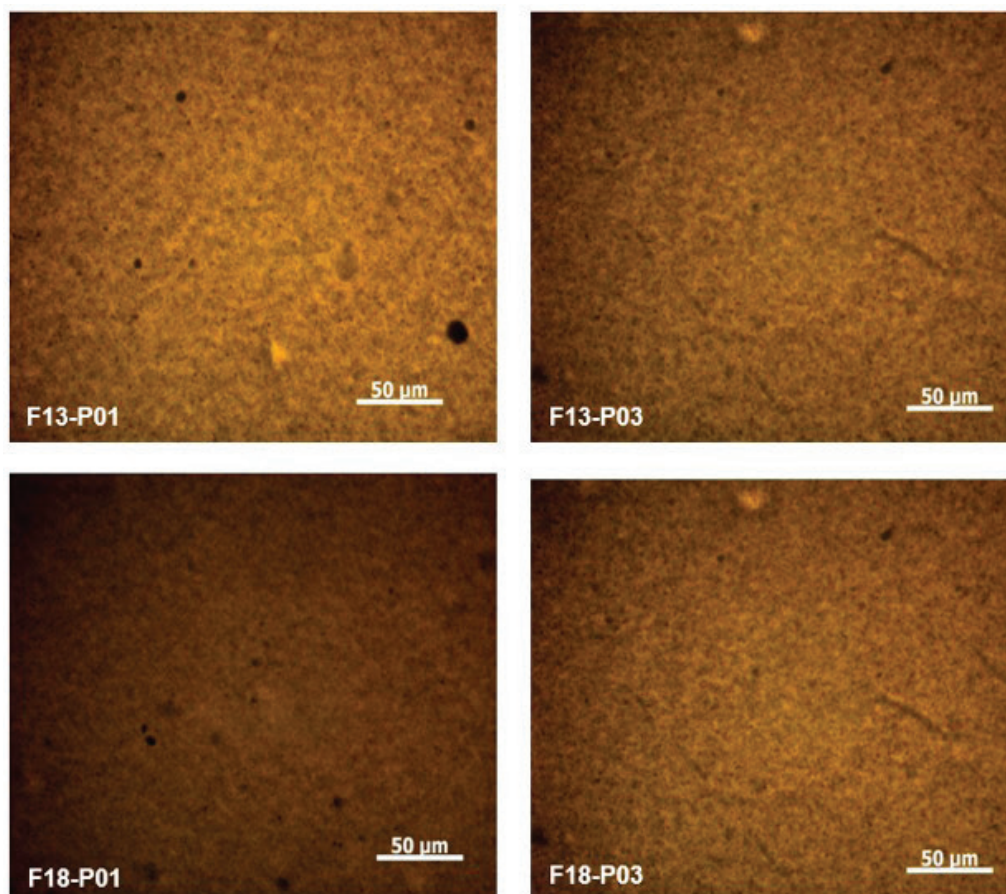
Figure 6. Comparative optical micrographs (OM) of F13 and F18 group, with 400X magnification.

4. Conclusions

The trimodal mixture and distribution of different CB can produce an optimized combination between these pigments to improve the colorimetric properties, with less interference in the rheological and processing characteristics of the polymer, compared to using a single particle. In this study, the formulations **F18 (25/75/00)** and **F13 (75/00/25)** were processed with different levels of specific mechanical energy **(SME)**, modulated by the screw rotation speed (N) and the feed rate (Q). It was determined that the higher energy level, in this case, 0.29 kWh/kg, brought an increase in tinting Strength, which went from 126.7% to 133.2% in the F18-P03, maintaining the viscosity due to the better dispersion of the pigment in the matrix, which was also detected in the complex viscosity. On the other hand, the F13-P03, due to the higher energy, improved its performance, slightly increasing the tinting strength from 113.9% to 124.8%. However, the MFI reduced from 29.7 g/10min to 7.2 g/10min, also observed in the rheological curves, demonstrating an increase in viscosity, compared to the previous study, due to the better dispersion of the pigment. Based on these results, it was possible to define the best process, with an SME of **0.29 kWh/kg** using **600 rpm** of rotation and **10 kg/h** of feed rate, for the F18-P03.

5. Author's Contribution

- **Conceptualization** – Juliano Martins Barbosa; Luiz Antonio Pessan.
- **Data curation** – Juliano Martins Barbosa; Luiz Antonio Pessan.
- **Formal analysis** – Juliano Martins Barbosa; Cesar Augusto Gonçalves Beatrice; Luiz Antonio Pessan.
- **Funding acquisition** – NA.
- **Investigation** – Juliano Martins Barbosa; Luiz Antonio Pessan.
- **Methodology** – Juliano Martins Barbosa; Cesar Augusto Gonçalves Beatrice; Luiz Antonio Pessan.
- **Project administration** – Juliano Martins Barbosa; Luiz Antonio Pessan.
- **Resources** – Juliano Martins Barbosa; Cesar Augusto Gonçalves Beatrice.
- **Software** – NA.
- **Supervision** – Juliano Martins Barbosa; Luiz Antonio Pessan.
- **Validation** – Juliano Martins Barbosa; Luiz Antonio Pessan.

- **Visualization** – Juliano Martins Barbosa; Luiz Antonio Pessan.
- **Writing – original draft** – Juliano Martins Barbosa; Luiz Antonio Pessan .
- **Writing – review & editing** – Juliano Martins Barbosa; Cesar Augusto Gonçalves Beatrice; Luiz Antonio Pessan.

6. Acknowledgements

7. References

1. Rabelo, M. S. (2000). *Aditivação de polímeros*. São Paulo: Artliber.

2. Callister, W. D., Jr. (2002). *Ciência e engenharia dos materiais: uma introdução*. Rio de Janeiro: LTC.

3. Donnet, J.-B. (Ed.). (1993). *Carbon black: science and technology* (2nd ed.). New York: Routledge. http://dx.doi.org/10.1201/9781315138763.

4. Penta Carbon. (2020, November 11). Retrieved in 2022, May 7, from https://pentacarbon.de/es/wiki/

5. Pfaff, G. (2021). Carbon black pigments. *Journal Physical Sciences Reviews*, *7*(2), 109-125. http://dx.doi.org/10.1515/psr-2020-0152.

6. Carbon Black Association. (2016). *Carbon black user's guide.* USA: Carbon Black Association. Retrieved in 2022, May 7, from http://www.cabotcorp.de/~/media/files/product-stewardship/industry-user-guides/international-carbon-black-association-icba-user-guide-portuguese.pdf

7. American Society for Testing and Materials – ASTM. (2014). *ASTM D3849-14a: standard test method for carbon black: morphological characterization of carbon black using electron microscopy.* West Conshohocken: ASTM. http://dx.doi.org/10.1520/D3849-14A.

8. American Society for Testing and Materials – ASTM. (2021). *ASTM D6556-21: standard test method for carbon black: total and external surface area by nitrogen adsorption.* West Conshohocken: ASTM. http://dx.doi.org/10.1520/D6556-21.

9. American Society for Testing and Materials – ASTM. (2018). *ASTM D2414-18: standard test method for carbon black: oil absorption number (OAN).* West Conshohocken: ASTM. http://dx.doi.org/10.1520/D2414-18.

10. Spahr, M. E., & Rothon, R. (2015). *Carbon black as a polymer filler.* In S. Palsule (Ed.), *Encyclopedia of polymers and composites* (pp. 1-24). Berlin: Springer. http://dx.doi.org/10.1007/978-3-642-37179-0_36-1.

11. Aghajan, M. H., Hosseini, S. M., & Razzaghi-Kashani, M. (2019). Particle packing in bimodal size carbon black mixtures and its effect on the properties of styrene-butadiene rubber compounds. *Polymer Testing*, *78*, 106002. http://dx.doi.org/10.1016/j.polymertesting.2019.106002.

12. Bretas, R. E. S., & D'Avila, M. A. (2000). *Reologia de polímeros fundidos.* São Carlos: EdUFSCar.

13. Aoki, Y., Hatano, A., & Watanabe, H. (2003). Rheology of carbon black suspensions. I.Three types of viscoelastic behavior. *Rheologica Acta*, *42*(3), 209-216. http://dx.doi.org/10.1007/s00397-002-0278-3.

14. Zhang, J.-F., & Yi, X.-S. (2002). Dynamic rheological behavior of high-density polyethylene filled with carbon black. *Journal of Applied Polymer Science*, *86*(14), 3527-3531. http://dx.doi.org/10.1002/app.11101.

15. American Society for Testing and Materials – ASTM. (2021). *ASTM D1765-21: standard classificationsystem for carbon blacks used in rubber products.* West Conshohocken: ASTM. http://dx.doi.org/10.1520/D1765-21.

16. Cabot Corporation. (2021, February 5). Retrieved in 2022, May 7, from https://www.cabotcorp.com/solutions/applications/plastics

17. Braskem. (2021, April 19). Retrieved in 2022, May 7, from https://www.braskem.com/busca-de-produtos?p=133

18. Domenech, T., Peuvrel-Disdier, E., & Vergnes, B. (2013). The importance of specific mechanical energy during twin screw extrusion of organoclay based polypropylene nanocomposites. *Composites Science and Technology*, *75*, 7-14. http://dx.doi.org/10.1016/j.compscitech.2012.11.016.

19. Dreiblatt, A. (2018). *Torque VS specific energy* [Webinar]. Century Extrusion Group. Retrieved in 2022, May 7, from https://ekc.cpmextrusiongroup.com/project/torque-vs-specific-energy/

20. Manas, I., & Tadmor, Z. (Ed.). (1994). *Mixing and compounding of polymers: theory and practice*. USA: Hanser Publishers.

21. Lotti, C., Isaac, C. S., Branciforti, M. C., Alves, R. M. V., Liberman, S., & Bretas, R. E. S.. (2008). Rheological, mechanical and transport property of blow films of high density polyethylene nanocomposites. *European Polymer Journal*, *44*(5), 1346-1357. http://dx.doi.org/10.1016/j.eurpolymj.2008.02.014.

22. American Society for Testing and Materials – ASTM. (2020). *ASTM D1603-20: standard test method for carbon black content in olefin plastics.* West Conshohocken: ASTM. http://dx.doi.org/10.1520/D1603-20.

23. American Society for Testing and Materials – ASTM. (2013). *ASTM D1238-13: standard test method for melt flow rates of thermoplastics by extrusion plastometer.* West Conshohocken: ASTM. http://dx.doi.org/10.1520/D1238-13.

24. Datacolor Color Measurement Instruments & Software. (2021, April 4). Retrieved in 2022, May 7, from https://www.datacolor.com/business-solutions/product-overview

25. Sarantópoulos, C. I. G. L., Oliveira, L. M., Padula, M., Coltro, L., & Alves, R. M. V. (2002). *Embalagens plásticas flexíveis: principais polímeros e avaliação das propriedades.* Campinas: CETEA/ITAL.

26. Byk Instruments. (2021, May 14). *Haze-gard transparency transmission haze meter*. Retrieved in 2022, May 7, from https://www.byk-instruments.com/en/Appearance/haze-gard-Transparency-Transmission-Haze-Meter/c/2345

27. American Society for Testing and Materials – ASTM. (2013). *ASTM D1003-13: standard test method for haze and luminous transmittance of transparent plastics.* West Conshohocken: ASTM. http://dx.doi.org/10.1520/D1003-13.

28. British Standards Institution – BSI. (2005). *BS EN 13900-5:2005: pigments and extenders: methods of dispersion and assessment of dispersibility in plastics - part 5: determination by filter pressure value test.* Belgium: BSI. http://dx.doi.org/10.3403/30105254U.